Rheological Performance of Bio-Char Modified Asphalt with Different Particle Sizes

Ran Zhang [1,2], Qingli Dai [2,*], Zhanping You [2,*], Hainian Wang [1,*] and Chao Peng [2,3]

1   School of Highway, Chang'an University, South Erhuan Middle Section, Xi'an 710064, China;
     ranzhang@mtu.edu
2   Department of Civil and Environmental Engineering, Michigan Technological University,
     1400 Townsend Drive, Houghton, MI 49931, USA; pengchao@cug.edu.cn
3   Faculty of Engineering, China University of Geosciences, Wuhan 430074, China
*   Correspondence: qingdai@mtu.edu (Q.D.); zyou@mtu.edu (Z.Y.); wanghnchd@gmail.com (H.W.);
     Tel.: +1-(906)-487-2620 (Q.D.); +1-(906)-370-0826 (Z.Y.); +86-(029)-8233-4432 (H.W.)

Abstract: To improve the performance of petroleum asphalt, bio-char was used as a modifier for a petroleum asphalt binder, in this study. The rheological properties of bio-char modified asphalt binders were compared with different particle sizes and contents, with one control and one flake graphite modified asphalt binder. Specifically, the bio-char modifiers with two particle sizes (ranging from 75 μm–150 μm and less than 75 μm) and three contents of 2%, 4%, and 8% were added into the asphalt binder. A flake graphite powder with particle sizes less than 75 μm was used as a comparison modifier. The Scanning Electron Microscopy (SEM) image showed the porous structure and rough surface of bio-char as well as dense structure and smooth surface of flake graphite. A Rotational Viscosity (RV) test, Dynamic Shear Rheometer (DSR) test, aging test, and Bending Beam Rheometer (BBR) test were performed to evaluate the properties of bio-char modified asphalt in this study. Both modifiers could improve the rotational viscosities of the asphalt binders. The porous structure and rough surface of bio-char lead to larger adhesion interaction in asphalt binder than the smooth flake graphite. As a result, the bio-char modified asphalts had better high-temperature rutting resistance and anti-aging properties than the graphite modified asphalt, especially for the binders with the smaller-sized and higher content of bio-char particles. Furthermore, the asphalt binder modified by the bio-char with sizes less than 75 μm and about 4% content could also achieve a better low-temperature crack resistance, in comparison to other modified asphalt binders. Thus, this type of bio-char particles is recommended as a favorable modifier for asphalt binder.

Keywords: bio-char; asphalt; modified asphalt; microscopic morphology; rheological properties; anti-aging properties

1. Introduction

Bio-char has been studied since the 20th century [1]. It is a product rich in carbon consisting of organic compounds, generally produced by pyrolysis technology [2,3]. The pyrolysis process is the biomass decomposition under free oxygen, with the products of gas, liquid (bio-oil) and solid (bio-char) [4,5]. There are various processes for pyrolysis: fast pyrolysis, slow pyrolysis, carbonization, and gasification according to the heating temperature and residence time [6–9]. The yield of by-products depends on the conditions of pyrolysis process, including heating temperature, heating rate, residence time, condensate rate and so on [10–13]. More bio-char can be produced within 400–500 °C, while the pyrolysis temperatures above 700 °C benefit the production of bio-based liquid and gas. The pyrolysis process occurs faster at high temperatures, usually taking a few seconds instead

of a few hours. Typical yields at high-temperature conditions include 60% bio-oil, 20% bio-char and 20% gases. In contrast, a higher yield of bio-char can be produced through slow pyrolysis, nearly a 50% yield [14].

The majority of studies on bio-char have been focused on its ability to act as an amendment for soil, to increase the soil productivity and to enhance the nutrient cycling and plant growth [15–18]. However, according to studies in recent years, it has been found that in some cases, the crop productivity cannot be increased and could even decrease because of the sorption of pesticides and water [19]. The use of bio-char in soil has a negative impact on the environment. It can lead to a detrimental impact on Greenhouse Gas (GHG) levels and the environment [20]. Bio-char can act as a sink of soil pollutants. Various toxic substances can be retained by bio-char through sorption or physicochemical reactions. Moreover, bio-char is difficult to be separated again from the soil, after its inactivation [19,21]. Currently, as one of the biomass pyrolysis waste by-products, bio-oil can get efficient use as a biofuel [11,22–24]. Along with bio-oil, bio-char is also produced as another byproduct, and if it cannot be used appropriately, and is instead randomly stacked, the bio-char in the air will also be a health risk for humans [25].

It is likely that bio-char can be used as a modifier for asphalt modification, to reduce environmental impacts and human health concerns. Meanwhile, carbon-based materials, such as carbon fiber, graphite, and carbon black, have been successfully applied in asphalt modification. With the addition of carbon fiber, the high-temperature properties and rutting resistance of asphalt binder, as well as the alleviation of the aging and oxidation processes, were improved [26,27]. Moreover, the fatigue life could be increased with the action of carbon nano-fiber [28]. The combination filler of graphite and carbon fiber improved the electrical property and the mechanical performance of asphalt concrete [29]. Carbon black could also be used to increase the anti-aging property, high-temperature performance and thermal conductivity of asphalt binder [30]. In addition, there has been a limited number of studies, over the past few years, about the application of bio-char as a construction and building material. A 1 wt% bio-char generated from food waste was found to increase the impermeability of mortar [31]. A pulp and paper mill sludge bio-char, with a content of 0.1% of total volume, was found to improve the mechanical strength of conventional concrete [32]. A 10 wt% swine manure bio-char decreases the temperature susceptibility and shear susceptibility of asphalt binder [33]. A 10 wt% switchgrass bio-char also significantly reduces the temperature susceptibility of asphalt binder and increases the moisture, cracking and rutting resistance of asphalt mixture [34,35].

Overall, a limited number of studies have focused on the performance evaluation of modified asphalt by using bio-char from waste wood as a modifier. Moreover, the application of bio-char as a pavement material can not only reduce the environmental pollution caused by bio-char but can also achieve the reuse of waste biomass sources. Motivated by these, the rheological properties of asphalt binder modified by bio-char, with different particle sizes, were evaluated in this study.

2. Motivation and Objectives

In order to seek a performance-favorable modifier, this study made a comprehensive investigation of the properties of asphalt binder modified by bio-char (different size ranges and contents) and flake graphite. The rheological properties were evaluated in the laboratory, and the effect of microscopic morphology, the particle size and the content of bio-char in the properties of bio-char modified asphalt binder, were researched in this study. Performance grade petroleum asphalt PG 58-28 and asphalt modified by commercial flake graphite were selected for comparison, in this study.

3. Materials and Preparation

3.1. Control Asphalt PG 58-28

The performance grade asphalt, PG 58-28, was one of the control binders in this study. It was obtained from Detroit, Michigan in the United States. The detailed properties of PG 58-28 are shown in Table 1. The test results all met the requirement of the specification [36].

Table 1. The properties of performance grade asphalt PG 58-28.

Test Properties	Test Results	Requirement of Specification
Specific gravity	1.03	–
Rotational viscosity @135 °C (Pa·s)	0.350	<3.0
G*/sinδ @ 58 °C for original binder (kPa)	1.995	>1.0
G*/sinδ @ 58 °C for RTFO binder (kPa)	5.018	>2.2

3.2. Graphite and Preparation of Graphite Modified Asphalt

Graphite was used in this study for comparison. The particle size of graphite was less than 75 μm and its density was 2.25 g/cm^3. The minimum thickness of the flake graphite layer was 0.11 mm [37]. The graphite was added to the base asphalt PG 58-28, based on the selected weight percentage of 4%, and was mixed by a high-speed shearing mixer, at 120 °C for approximately 1 h.

3.3. Bio-Char and Preparation of Bio-Char Modified Asphalt

The bio-char was supplied by an energy company. It was generated from waste wood resources, at temperatures ranging from 500–650 °C, through the pyrolysis technology, with a high heating rate of 104–105 °C/s. The bio-char particles were sieved to separate the different size ranges of particles. Only smaller particle sizes of bio-char were used in this study to achieve homogeneous and uniform mixing. The specific particle sizes of bio-char ranging from 75 μm–150 μm and less than 75 μm, were chosen in this study. The bio-char contents were 2%, 4% and 8% by weight of the total asphalt and its density was about 0.4 g/cm^3, in this study. The bio-char was added into the base asphalt PG 58-28, based on the selected weight percentages, by a high-speed shearing mixer, at 120 °C for approximately 1 h.

Petroleum asphalt PG 58-28 sample and graphite modified asphalt sample were used in this study, for comparison purposes. As can be seen in Table 2, a total of seven bitumen blended with additives and one original binder of PG 58-28 were produced. In this research, 'B' stands for bio-char, 'G' stands for graphite, 'L' for larger particle size, and 'S' for smaller particle size.

Table 2. Sample range matrix.

Binder Types	Modifier Type	Modifier Content (wt %)	Particle Size
PG58-28	N/A	N/A	N/A
2% BL	Bio-char	2	75 μm < d < 150 μm
4% BL	Bio-char	4	75 μm < d < 150 μm
8% BL	Bio-char	8	75 μm < d < 150 μm
2% BS	Bio-char	2	d < 75 μm
4% BS	Bio-char	4	d < 75 μm
8% BS	Bio-char	8	d < 75 μm
4% GS	Graphite	4	d < 75 μm

4. Experimental Program

4.1. Scanning Electron Microscopy (SEM) Test

SEM test was applied to obtain the microscopic morphology of materials [38]. In this study, the SEM test was conducted by a Hitachi (Schaumburg, IL, USA) S-4700 and JEOL (Peabody, M, USA)-6400. The bio-char or graphite particles were dispersed onto double-sided adhesive carbon

tape, which was applied to the aluminum sample mounts. For the operation of Hitachi S-4700, the accelerating voltage was 1–5 kV, the emission current was 9 A, and the working distance was 2.8–8 mm. For the operation of JEOL-6400, the accelerating voltage was 20 kV and the working distance was 39 mm. The bio-char and graphite samples were coated with a carbon thin film.

4.2. Rotational Viscosity (RV) Test

The rotational viscosity test was applied to measure the asphalt's resistance to flow and the workability of asphalt binders. The viscosity measurements were conducted on asphalt by a Brookfield Rotational Viscometer following the American Association of State Highway and Transportation Officials (AASHTO) Designation: T 316-13 [39]. The test temperatures were: 90 °C, 110 °C, 135 °C, 150 °C, and 165 °C, respectively, and the shear rate was set at 20 r/min. Three replicates were used for each type of asphalt sample.

4.3. Dynamic Shear Rheometer (DSR) Test

The Dynamic Shear Rheometer (DSR) test can be conducted to determine the rheological behavior of asphalt binders in varying temperature and frequency conditions [40,41]. The asphalt PG 58-28, graphite modified asphalt and bio-char modified asphalts were tested by the DSR in the original RTFO (Rolling Thin-Film Oven)-aged and PAV (Pressurized Aging Vessel)-aged states. The test temperatures chosen for the original and the RTFO-aged asphalt were, 52 °C, 58 °C, 64 °C, 70 °C, and 76 °C, to characterize the rutting resistance. The test temperatures were 13 °C, 19 °C, 25 °C, 31°C, and 37 °C, for PAV-aged asphalt binders. A water bath was used to control the temperature. The AASHTO T315 [42] test procedure was followed for the DSR test. Three replicates were used for each type of asphalt sample.

4.4. Aging Test

The RTFO test and PAV test were conducted for asphalt binders. The RTFO test and the PAV test were applied to simulate the aging of asphalt binder, during the process of construction and its service life, respectively [7,43]. In the standard RTFO test, the binders were conditioned at 163 °C, for 85 min, with sufficient air. The procedures of the standard RTFO test followed the AASHTO T240 [44]. Then, the RTFO-aged samples were used for the PAV test, under an air pressure of 2.1 MPa, for 20 h, based on the AASHTO R28 [45].

4.5. Bending Beam Rheometer (BBR) Test

The Bending Beam Rheometer (BBR) test was used for the evaluation of the rheological and thermal cracking properties of asphalt binders. The specific operation process of this test was based on AASHTO standard T 313-12 [46]. The results of the BBR test could be applied to indicate the resistance to cracking in asphalt binders, at low temperatures. The asphalt samples were aged by the PAV test before the BBR test. The test temperature was controlled to be kept at the low temperature of −18 °C, by using an ethanol fluid. Moreover, stiffness was calculated based on Equation (1) [47].

$$S_t = (PL^3)/(4bh^3\delta_t) \tag{1}$$

where

P—Applied constant load (100 g or 0.98 N);
L—Distance between beam supports (102 mm);
b—Beam width (12.5 mm);
h—Beam thickness (6.25 mm);
S_t—Asphalt binder stiffness at a specific time;
δ_t—Deflection at a specific time.

5. Results and Discussions

5.1. Microscopic Morphology Analysis

The microscopic morphologies of graphite and bio-char were observed by using the SEM test. The images of graphite and bio-char, magnified by the SEM, are shown in Figure 1.
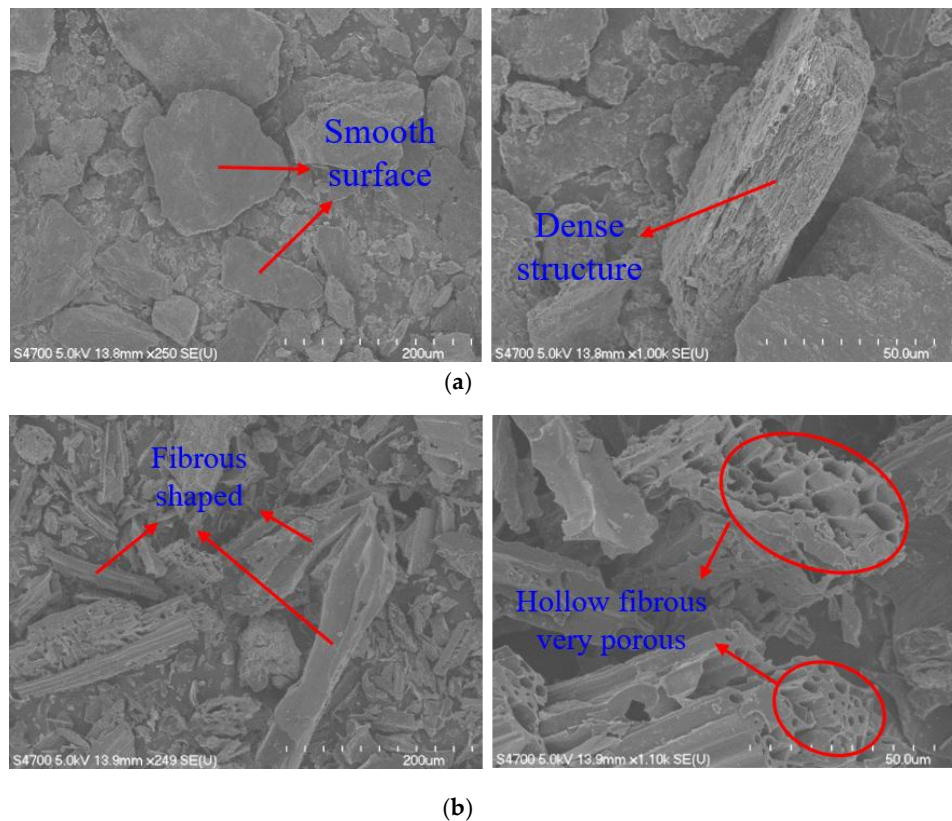

Figure 1. (**a**) Images of graphite magnified by SEM; (**b**) images of bio-char magnified by SEM.

It could be seen that the flake graphite and the bio-char had different structures and surface textures. The flake graphite had a smooth surface texture. Meanwhile, graphite had a dense microscopic morphology, that could be determined on the basis of Figure 1, and had a higher density of 2.25 g/cm^3. The bio-char was irregular hollow fibrous particles and had a very porous structure. The bio-char had a more complex and rough surface texture than the graphite. The hollow, fibrous, porous structure, and rough surface texture led the bio-char to have a higher surface area, which then led to a larger adhesion interaction, in the asphalt. Therefore, the special microscopic morphology of bio-char, the hollow, fibrous, porous structure and rough surface texture, might have contributed to the form of a strong biochar-binder matrix structure [34]. This might have led the bio-char modified asphalts to have a better resistance to deformation, at high temperatures. Meanwhile, the solid particles of bio-char and graphite were stiff particles. The addition of bio-char and graphite particles might have stiffened the asphalt binder to some degree.
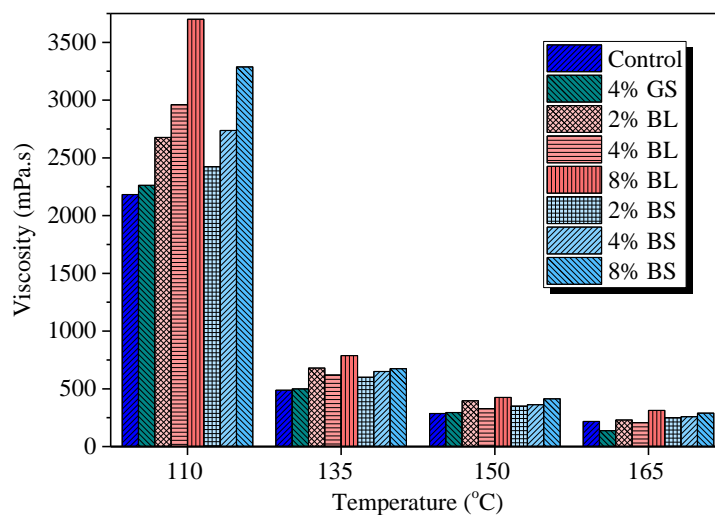
5.2. Rotational Viscosity Test

5.2.1. Rotational Viscosity Analysis

The rotational viscosities of asphalt binders before and after RTFO aging, are shown in Figure 2a,b, respectively.
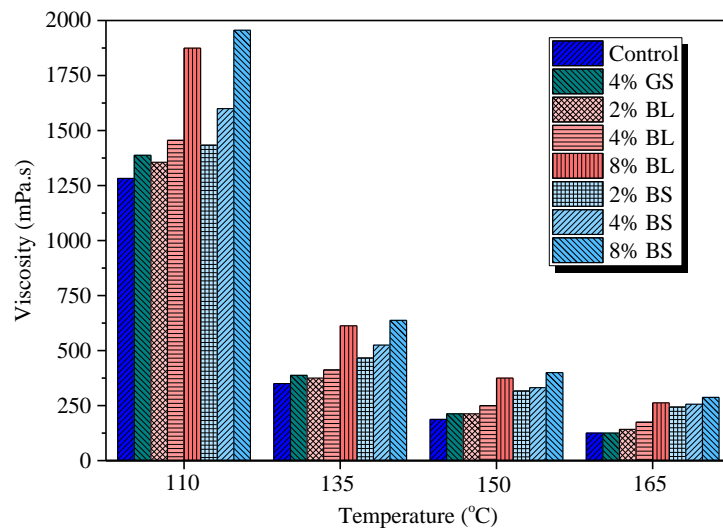
(**a**)

(**b**)

Figure 2. (**a**) Rotational viscosities of original control, graphite modified and bio-char modified asphalts; (**b**) rotational viscosities of control, graphite modified and bio-char modified asphalts after RTFO aging.

From Figure 2a, it is noteworthy that all the asphalt binders could satisfy the specification requirement for the rotational viscosity of no more than 3000 mPa·s, at 135 °C. The addition of the graphite or the bio-char contributed to the increase of rotational viscosities of the asphalt binders. As the bio-char content increased, the rotational viscosities of the bio-char modified asphalts had an increasing trend. For example, the rotational viscosities of 4% GS, 2% BL, 4% BL and 8% BL increased by an average of 8.06%, 9.90%, 26.19%, and 82.81%, respectively, as compared with the control asphalt binder at 110–165 °C. However, the increased value was smaller when the bio-char content was lower. For example, the rotational viscosities of 2% BL and 2% BS were only higher than that of the control asphalt binder by 25 mPa·s and 116.6 mPa·s, respectively. These could be explained by the stiffening influence from the increasing concentration of stiff particles. The addition of bio-char or graphite increased the concentration of stiff particles in asphalt and contributed to the increase of elastic components, which accordingly increased the viscosity of the asphalt binder. The bio-char size

had an effect on the rotational viscosities of bio-char modified asphalt. At 135 °C, the viscosities of 2% BS, 4% BS, and 8% BS were higher than 2% BL, 4% BL, and 8% BL by 91.7 mPa·s, 112.5 mPa·s, and 25.0 mPa·s, respectively (Figure 2a). This illustrated that bio-char modified asphalt binders with smaller-sized particles had higher viscosities than those with larger-sized particles. Furthermore, the bio-char modified asphalts had higher viscosities compared to the graphite modified asphalt binder. The rotational viscosities of 4% BL and 4% BS were higher than that of 4% GS, by 17.26% and 52.93%, on average, respectively. Under the same dosage, the bio-char had a higher volume and surface area than the graphite because of its lower density and porous structure. Moreover, the smaller-sized bio-char particles had a higher number of particles than the larger-sized ones, thereby, this also led to a higher surface area. The higher surface area and porous structure of bio-char led to a larger adhesion interaction in the base asphalt binder, which lowered the fluidity of asphalt binder and increased the viscosity.

After RTFO aging (Figure 2b), all the asphalt binders had higher viscosities than the original asphalt binders, because of the oxidation of the asphalt binders [48,49]. However, all the rotational viscosities of asphalt binders were still far less than 3 Pa·s. The obvious change was that the viscosity differences of the bio-char modified asphalts, with different bio-char contents, were lower than those before the RTFO aging had. When unaged, the viscosities of 4% BS and 8% BS were higher than 2% BS by 8.44% and 29.31%, on average, respectively. But after the RTFO aging, the viscosities of 4% BS and 8% BS were higher than 2% BS by 7.03% and 20.58%, on average, respectively. This indicated that the bio-char modified asphalts had different age degrees.

5.2.2. Anti-Aging Property Analysis

To further compare the anti-aging properties of different asphalt binders, the aging index was applied, in this study. The aging index was obtained from Equation (2).

$$I_{ag}{}^r = V_{RTFO}/V_{origin} \tag{2}$$

where

$I_{ag}{}^r$—Aging index of the asphalt binder;
V_{RTFO}—Rotational viscosity of RTFO aged asphalt binder;
V_{origin}—Rotational viscosity of the original asphalt binder.

The aging indexes of all asphalt binders, at 135 °C, were calculated and are displayed in Figure 3. The higher the aging index, the worse the anti-aging property of asphalt binder was found to be. The aging indexes of 2% BS, 4% BS, and 8% BS decreased by 29.13%, 17.58, and 17.65% more than those of 2% BL, 4% BL, and 8% BL, respectively. This illustrated that as the bio-char content increased, the anti-aging properties of bio-char modified asphalts increased. This could be explained by the stiffening effect caused by the high content of bio-char, which reduced the aging effects. Meanwhile, the bio-char modified asphalts with smaller-sized particles had better anti-aging properties than those with larger-sized particles. At the same content, the smaller-sized bio-char led to higher numbers of stiff particles, as a result, the aging effects were more likely to be suppressed with this stronger stiffening effect. Moreover, 2% BS, 4% BS, and 8% BS had higher anti-aging property compared to the control asphalt binder. In addition, the 4% BS had a better anti-aging property than 4% GS. The bio-char had lower density and higher volume than graphite, at the same dosage. On one hand, this could be explained by the higher volume filling, which decreased the oxidation. On the other hand, the complex fibrous and porous structure of bio-char might have led to larger adhesion interaction between the bio-char and the base asphalt binder molecules, and thus decreased the oxidation.
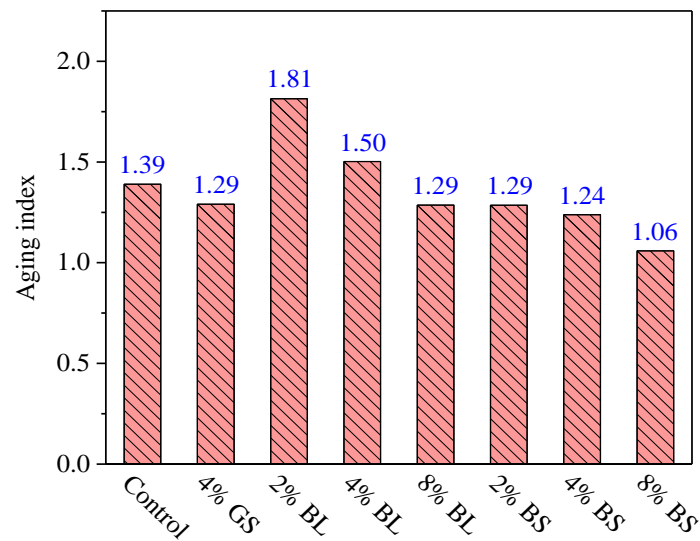
Figure 3. Aging indexes of control, graphite modified and bio-char modified asphalts.

*5.3. Dynamic Shear Rheometer Test*

5.3.1. Rutting Resistance Analysis

From Figure 4a, the rutting indexes of 2% BL, 4% BL, 8% BL, 2% BS, 4% BS, and 8% BS increased by 4.55%, 17.49%, 45.72%, 23.61%, 31.70%, and 58.40%, on average, as compared to that of the control asphalt binder within a 52 °C to 76 °C temperature range. This meant that bio-char modified asphalts had better resistance to rutting at higher temperatures than the control asphalt binder. This was partially attributed to the stiff volume-filling particles, such as the bio-char particles. The other reason might be that the porous structure of bio-char led to a higher surface area which, accordingly, led to the higher adhesion between the bio-char and the base asphalt binder. With the increasing of bio-char content, the rutting resistance became stronger. The enforcement of interaction among the bio-char particles might be a contributor to the higher rutting resistance. With the increase of bio-char content, stiff porous particles came into contact with each other, and a skeleton framework could be formed when the bio-char content increased to a higher amount. The higher rutting resistance also could be explained by the higher viscosity. The conclusions were consistent with the above conclusions about the viscosities.

From Figure 4b, after the RTFO aging, the rutting indexes of bio-char modified asphalts were higher than those before RTFO aging, because of the aging. Additionally, the bio-char modified asphalts still had higher aging resistance than the control asphalt binder. It was evident that bio-char modified asphalts, with larger-sized particles, had a more obvious change than those with smaller-sized particles. The rotational viscosities of 2% BL, 4% BL, and 8% BL were 5.80%, 3.09%, and 4.16% higher than those of 2% BS, 4% BS, and 8% BS, respectively, after the RTFO aging, while they were 15.36%, 10.76%, and 8.01% lower, respectively, before the RTFO aging. This could be attributed to the relatively weak aging resistance of bio-char modified asphalts with larger particle sizes. These conclusions were consistent with the above conclusions about the anti-aging properties.
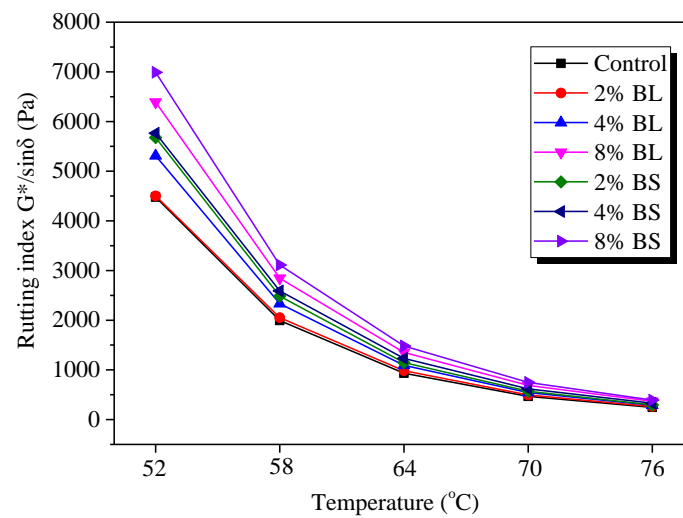
(**a**)
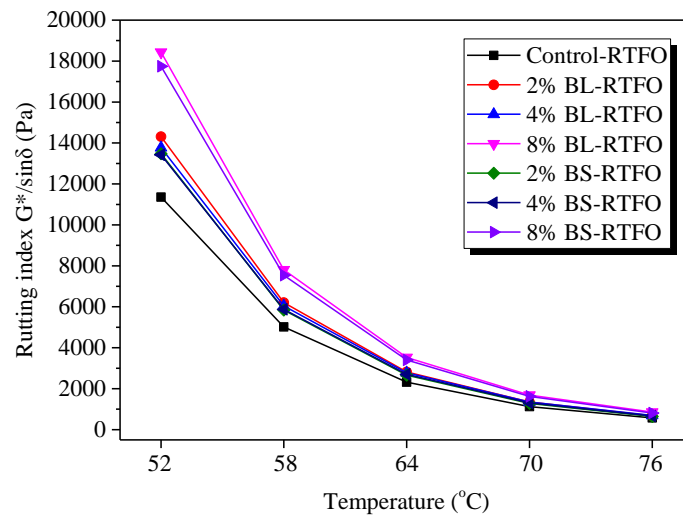
(**b**)

Figure 4. (**a**) Rutting indexes (G*/sinδ) of original control and bio-char modified asphalts; (**b**) rutting indexes (G*/sinδ) of control and bio-char modified asphalts after RTFO aging.

The rutting indexes of the control asphalt binder, 4% GS, 4% BL, and 4% BS, before and after RTFO aging, are displayed in Figure 5. Before the RTFO aging, the rutting indexes of 4% GS, 4% BL, and 4% BS increased by 2.32%, 17.49%, and 31.70%, on average, compared to that of the control asphalt. Therefore, the graphite modified asphalt had a similar rutting index to that of the control asphalt, and bio-char modified asphalt has better rutting index than that of the graphite modified asphalt. After the RTFO aging, the rutting indexes of 4% GS, 4% BL, and 4% BS increased by 7.07%, 20.59%, and 16.98%, on average, compared to that of the control asphalt binder. This indicated, to a large extent, that the bio-char modified asphalts had better aging resistance than the graphite modified asphalt, especially, for the bio-char modified asphalt with smaller-sized particles. The higher number of stiff particles and the fibrous and porous structure of the bio-char contributed to the form of a biochar-binder matrix.
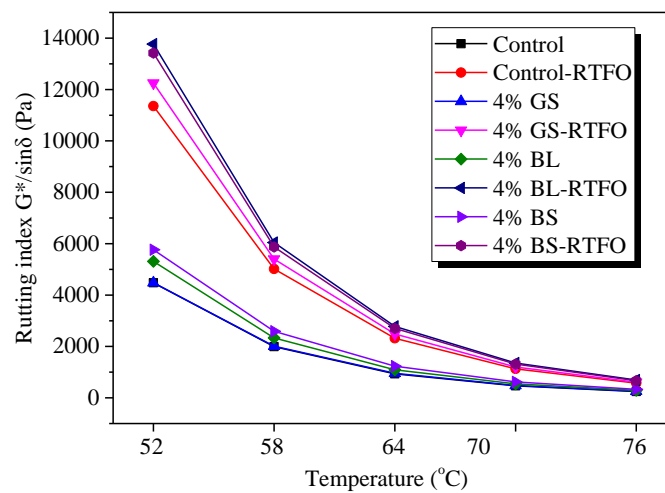
Figure 5. Rutting indexes (G*/sinδ) of different types of asphalt binders.

5.3.2. High Critical Temperature Analysis

According to the Superpave TM specification, the high critical temperature of asphalt is the temperature at which the rutting index at 1.59 Hz (10 rad/s) is 1.0 KPa for the unaged asphalt, and is 2.2 KPa for the RTFO aged asphalt. The high critical temperatures of asphalt binders were determined based on Equation 3, and the results are shown in Table 3. It is obvious that bio-char modified asphalts had better high-temperature properties than the control and graphite modified asphalts. The high critical temperatures of 4% GS, 4% BL, and 4% BS were higher than the control asphalt binder by 0.31 °C, 1.57 °C, and 2.92 °C, respectively. Moreover, the bio-char modified asphalts with smaller-sized particles had the best high-temperature properties. The bio-char has a lower density than graphite, therefore, the amount of stiff bio-char particles were higher as compared to that of graphite, at the same dosage. Furthermore, the smaller-sized bio-char particles had the highest number of stiff particles and the highest surface area. The porous structure and higher surface area might have played a significant role, which led to larger adhesion interaction in the asphalt binder, promoted the formation of a biochar-binder matrix and, thus, decreased the thermal influence [34].

$$T^{(G^*/\sin\delta)} = \text{Minimum} \left(T_o^{(G^*/\sin\delta)}, T_R^{(G^*/\sin\delta)}\right) \tag{3}$$

where

$T^{(G^*/\sin\delta)}$ = The high critical temperatures of asphalts;
$T_o^{(G^*/\sin\delta)}$ = The high critical temperatures of original asphalts;
$T_R^{(G^*/\sin\delta)}$ = The high critical temperatures of RTFO aged asphalts.

Table 3. The high critical temperatures of control, graphite modified, and bio-char modified asphalts.

	Control Asphalt	4% GS	2% BL	4% BL	8% BL	2% BS	4% BS	8% BS
$T_o(G^*/\sin\delta)$	63.56	63.87	63.90	65.13	67.07	65.76	66.48	68.03
$T_R(G^*/\sin\delta)$	64.61	65.18	66.62	66.34	68.21	65.91	66.22	68.09
$T(G^*/\sin\delta)$	63.56	63.87	63.90	65.13	67.07	65.76	66.48	68.03

5.4. Bending Beam Rheometer Test

5.4.1. Low-Temperature Cracking Resistance Analysis

The BBR test was conducted for all the asphalt binders, to evaluate their low temperature cracking resistance. Based on the Superpave TM specification, −18 °C is recommended for the test temperature.

And the specification requirement for the PAV-aged sample is the creep stiffness of less than 300 MPa and an m-value of higher than 0.3. The test results of creep stiffness and m-value for control, graphite modified, and bio-char modified asphalts are shown in Table 4.

The stiffness of 2% BL, 4% BL, 8% BL, 2% BS, 4% BS, and 8% BS was higher by −2 MPa, 64 MPa, 66 MPa, 34 MPa, 83 MPa, and 105 MPa, respectively, compared to the control asphalt. Though bio-char modified asphalts had higher creep stiffness than the control asphalt binder, they all satisfied the specification requirement of less than 300 MPa. The m-values of 4% BL, 8% BL, and 8% BS were 0.29, 0.28, and 0.28, respectively, which could not satisfy the requirements of the specification. As the bio-char content increased, the low-temperature properties of bio-char modified asphalts decreased. Therefore, there should have been a limit on the bio-char content of less than 4%. The reason is that stiff particles made the asphalt binder stiffer and more brittle, at low temperatures. This led to the smaller deformation capacity or compliance, according to the weak low-temperature properties. It could also be found that the bio-char particle size had an effect on the low-temperature performances, and the bio-char modified asphalts, with smaller-sized particles, had better low temperature cracking resistance than those with larger-sized particles. The m-values of 2% BS and 4% BS were 0.33% and 2.4% higher than those of 2% BL and 4% BL, respectively. The PAV-aged samples were used in the BBR test. This might have been caused by the more uniform distribution and interaction with the smaller stiff particles. Alternatively, the better anti-aging properties of bio-char modified asphalts, with smaller-sized particles, might have made the asphalt binder softer, and, thus, led to better cracking resistance at low temperatures. The m-values of 4% BS and 4% GS were both 0.30. This illustrated that bio-char modified asphalts had very similar low-temperature properties as that of the graphite asphalt binder, for the same particle sizes.

Table 4. The Bending Beam Rheometer (BBR) results of control, graphite modified and bio-char modified asphalts at −18°C.

Asphalt Binder	Time (s)	Deflection (mm)	Stiffness (mPa)	m-Value	Remarks (for Stiffness and m-Value)
Control	60.0	0.446	179	0.31	Pass the specification
4% GS	60.0	0.422	187	0.30	Pass the specification
2% BL	60.0	0.447	177	0.30	Pass the specification
4% BL	60.0	0.329	243	0.29	Fail the specification
8% BL	60.0	0.328	245	0.28	Fail the specification
2% BS	60.0	0.378	213	0.30	Pass the specification
4% BS	60.0	0.308	262	0.30	Pass the specification
8% BS	60.0	0.284	284	0.28	Fail the specification

5.4.2. Low Critical Temperature Analysis

The low critical temperature of asphalt was determined on the basis of the Superpave TM specification, in which the creep stiffness is 300 MPa and the m-value is 0.3 [36]. The low critical temperatures of all asphalts are shown in Figure 6.

From Figure 6, it could be seen that 4% BS had better low critical temperature than 4% GS. The 2% BL, 2% BS, and 4% BS had better low critical temperatures which were no higher than −18 °C. The bio-char content should have been less than 4% because the low critical temperatures of bio-char modified asphalts increased with the added bio-char, and the low critical temperatures of 8% BL and 8% BS were much higher than −18 °C. Furthermore, the low critical temperatures of 2% BS and 4% BS were lower than those of 2% BL and 4% BL. Therefore, the smaller bio-char particles size of less than 75 μm were recommended to be used as the modifier.
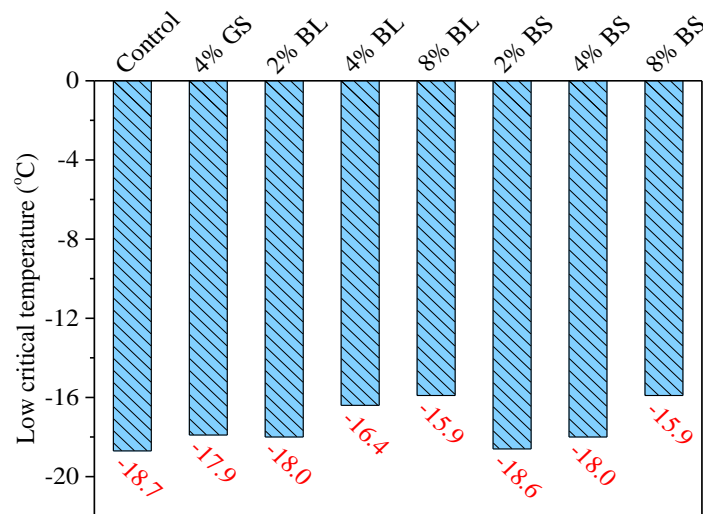
Figure 6. Low critical temperatures of control, graphite modified and bio-char modified asphalts.

6. Summaries and Conclusions

The bio-char was investigated as a favorable modifier to improve the rheological performance of asphalt binders. Bio-char with two particle size ranges of 75 μm–150 μm and less than 75 μm were used as the modifiers. The content of bio-char was 2%, 4%, and 8% respectively. The flake graphite with a size range of less than 75 μm and a content of 4% was utilized as a modifier of asphalt, for comparison. The Scanning Electron Microscopy characterization, Rotational Viscosity test, Dynamic Shear Rheometer test, and the Bending Beam Rheometer test were conducted to evaluate the modified binder performance. The conclusions obtained are as follows:

(1) Compared with dense and smooth flake graphite, the bio-char particle had a more porous microstructure and rough surface texture.

(2) Both bio-char and graphite could increase the rotational viscosity of the asphalt, with the added contents. The bio-char modified asphalt binders with smaller-sized particles had higher viscosities than those with larger-sized particles. They all satisfied the requirement for the specifications of rotational viscosity—less than or equal to 3000 mPa·s at 135 °C.

(3) The porous structure and rough surface of bio-char could lead to a larger adhesion interaction in asphalt binder than those of the smooth flake graphite. As a result, the bio-char modified asphalts had a better high-temperature rutting resistance and better anti-aging properties than that of the graphite modified asphalt. A more noticeable improvement was found for the bio-char modified asphalt with the smaller-sized and higher number of particles. Moreover, the bio-char modified asphalts with the smaller-sized particles had the highest critical temperatures among all other binder types.

(4) Though the crack resistance, at low temperatures, of the bio-char modified asphalts decreased with the added bio-char, as seen in the BBR test results, the low critical temperatures were still lower than −18 °C, with the smaller-sized bio-char particles. The bio-char modified asphalts had similar low-temperature properties as that of the graphite modified asphalt binder.

In summary, it is possible to use bio-char as a modifier for the petroleum asphalt binder. This study showed that the bio-char with a size range of less than 75 μm and a content of less than 4% could increase the anti-aging property and rutting resistance of the asphalt binder, as well as keep a good low-temperature crack resistance in the asphalt binder. Thus, this type of bio-char particles could be used as an environment-friendly and favorable modifier for the asphalt binder. In future studies, the porous structure of bio-char and the interface bonding between the bio-char and the asphalt will be investigated to facilitate this application.

References

1. Demirbas, A.; Pehlivan, E.; Altun, T. Potential evolution of Turkish agricultural residues as bio-gas, bio-char and bio-oil sources. *Int. J. Hydrogen Energy* **2006**, *31*, 613–620. [CrossRef]

2. Jaiswal, A.K.; Elad, Y.; Graber, E.R.; Frenkel, O. Rhizoctonia solani suppression and plant growth promotion in cucumber as affected by biochar pyrolysis temperature, feedstock and concentration. *Soil Biol. Biochem.* **2014**, *69*, 110–118. [CrossRef]

3. Muñoz, E.; Curaqueo, G.; Cea, M.; Vera, L.; Navia, R. Environmental hotspots in the life cycle of a biochar-soil system. *J. Clean. Prod.* **2017**, *158*, 1–7. [CrossRef]

4. Mohan, D.; Pittman, C.U.; Steele, P.H. Pyrolysis of wood/biomass for bio-oil: A critical review. *Energy Fuels* **2006**, *20*, 848–889. [CrossRef]

5. Zhong, Z.; Song, B.; Zaki, M. Life-cycle assessment of flash pyrolysis of wood waste. *J. Clean. Prod.* **2010**, *18*, 1177–1183. [CrossRef]

6. Zhang, R.; Wang, H.; You, Z.; Jiang, X.; Yang, X. Optimization of bio-asphalt using bio-oil and distilled water. *J. Clean. Prod.* **2017**, *165*, 281–289. [CrossRef]

7. Yang, X.; You, Z.-P.; Dai, Q.-L. Performance evaluation of asphalt binder modified by bio-oil generated from waste wood resources. *Int. J. Pavement Res. Technol.* **2013**, *6*, 431–439.

8. Imam, T.; Capareda, S. Characterization of bio-oil, syn-gas and bio-char from switchgrass pyrolysis at various temperatures. *J. Anal. Appl. Pyrolysis* **2012**, *93*, 170–177. [CrossRef]

9. Zhang, R.; Wang, H.; Jiang, X.; You, Z.; Yang, X.; Ye, M. Thermal storage stability of bio-oil modified asphalt. *J. Mater. Civ. Eng.* **2018**, *30*, 04018054. [CrossRef]

10. Gaunt, J.L.; Lehmann, J. Energy balance and emissions associated with biochar sequestration and pyrolysis bioenergy production. *Environ. Sci. Technol.* **2008**, *42*, 4152–4158. [CrossRef] [PubMed]

11. Zhang, R.; Wang, H.; Gao, J.; You, Z.; Yang, X. High temperature performance of sbs modified bio-asphalt. *Constr. Build. Mater.* **2017**, *144*, 99–105. [CrossRef]

12. Zhang, R.; Wang, H.; Gao, J.; Yang, X.; You, Z. Comprehensive performance evaluation and cost analysis of sbs-modified bioasphalt binders and mixtures. *J. Mater. Civ. Eng.* **2017**, *29*, 04017232. [CrossRef]

13. Zhao, B.; O'Connor, D.; Zhang, J.; Peng, T.; Shen, Z.; Tsang, D.C.; Hou, D. Effect of pyrolysis temperature, heating rate, and residence time on rapeseed stem derived biochar. *J. Clean. Prod.* **2018**, *174*, 977–987. [CrossRef]

14. Smith, J.L.; Collins, H.P.; Bailey, V.L. The effect of young biochar on soil respiration. *Soil Biol. Biochem.* **2010**, *42*, 2345–2347. [CrossRef]

15. Mukherjee, A.; Zimmerman, A.R. Organic carbon and nutrient release from a range of laboratory-produced biochars and biochar–soil mixtures. *Geoderma* **2013**, *193*, 122–130. [CrossRef]

16. Masiello, C.; Dugan, B.; Brewer, C.; Spokas, K.; Novak, J.; Liu, Z.; Sorrenti, G. Biochar effects on soil hydrology. In *Biochar for Environmental Management*, 2nd ed.; Routledge: Earthscan, UK, 2015.

17. Suliman, W.; Harsh, J.B.; Abu-Lail, N.I.; Fortuna, A.-M.; Dallmeyer, I.; Garcia-Pérez, M. The role of biochar porosity and surface functionality in augmenting hydrologic properties of a sandy soil. *Sci. Total Environ.* **2017**, *574*, 139–147. [CrossRef] [PubMed]

18. Ali, S.; Rizwan, M.; Qayyum, M.F.; Ok, Y.S.; Ibrahim, M.; Riaz, M.; Arif, M.S.; Hafeez, F.; Al-Wabel, M.I.; Shahzad, A.N. Biochar soil amendment on alleviation of drought and salt stress in plants: A critical review. *Environ. Sci. Pollut. Res.* **2017**, *24*, 12700–12712. [CrossRef] [PubMed]

19. Six, J. Biochar: Is There a Dark Side? 2014. Available online: https://www.ethz.ch/en/news-and-events/eth-news/news/2014/04/biochar-is-there-a-dark-side.html (accessed on 1 April 2014).

20. Downie, A. *Biochar Production and Use: Environmental Risks and Rewards*; University South Wales: Treforest, UK, 2011.

21. An, C.; Huang, G. Environmental concern on biochar: Capture, then what? *Environ. Earth Sci.* **2015**, *74*, 7861–7863. [CrossRef]

22. Yang, X.; You, Z.; Dai, Q.; Mills-Beale, J. Mechanical performance of asphalt mixtures modified by bio-oils derived from waste wood resources. *Constr. Build. Mater.* **2014**, *51*, 424–431. [CrossRef]

23. Fini, E.H.; Al-Qadi, I.L.; You, Z.; Zada, B.; Mills-Beale, J. Partial replacement of asphalt binder with bio-binder: Characterisation and modification. *Int. J. Pavement Eng.* **2012**, *13*, 515–522. [CrossRef]

24. Yang, X.; Mills-Beale, J.; You, Z. Chemical characterization and oxidative aging of bio-asphalt and its compatibility with petroleum asphalt. *J. Clean. Prod.* **2017**, *142*, 1837–1847. [CrossRef]

25. Brick, S.; Lyutse, S. *Biochar: Assessing the Promise and Risks to Guide US Policy*; NRDC Issue Paper; Natural Resources Defense Council: New York, NY, USA, 2010.

26. Cleven, M.A. *Investigation of the Properties of Carbon Fiber Modified Asphalt Mixtures*; Michigan Technological University: Houghton, MI, USA, 2000.

27. Yao, H.; You, Z.; Li, L.; Goh, S.W.; Lee, C.H.; Yap, Y.K.; Shi, X. Rheological properties and chemical analysis of nanoclay and carbon microfiber modified asphalt with fourier transform infrared spectroscopy. *Constr. Build. Mater.* **2013**, *38*, 327–337. [CrossRef]

28. Khattak, M.J.; Khattab, A.; Rizvi, H.R.; Zhang, P. The impact of carbon nano-fiber modification on asphalt binder rheology. *Constr. Build. Mater.* **2012**, *30*, 257–264. [CrossRef]

29. Liu, X.; Wu, S. Study on the graphite and carbon fiber modified asphalt concrete. *Constr. Build. Mater.* **2011**, *25*, 1807–1811. [CrossRef]

30. Cong, P.; Xu, P.; Chen, S. Effects of carbon black on the anti aging, rheological and conductive properties of sbs/asphalt/carbon black composites. *Constr. Build. Mater.* **2014**, *52*, 306–313. [CrossRef]

31. Gupta, S.; Kua, H.W.; Koh, H.J. Application of biochar from food and wood waste as green admixture for cement mortar. *Sci. Total Environ.* **2018**, *619*, 419–435. [CrossRef] [PubMed]

32. Akhtar, A.; Sarmah, A.K. Novel biochar-concrete composites: Manufacturing, characterization and evaluation of the mechanical properties. *Sci. Total Environ.* **2018**, *616*, 408–416. [CrossRef] [PubMed]

33. Walters, R.C.; Fini, E.H.; Abu-Lebdeh, T. Enhancing asphalt rheological behavior and aging susceptibility using bio-char and nano-clay. *Am. J. Eng. Appl. Sci.* **2014**, *7*, 66–76. [CrossRef]

34. Zhao, S.; Huang, B.; Ye, X.P.; Shu, X.; Jia, X. Utilizing bio-char as a bio-modifier for asphalt cement: A sustainable application of bio-fuel by-product. *Fuel* **2014**, *133*, 52–62. [CrossRef]

35. Zhao, S.; Huang, B.; Shu, X.; Ye, P. Laboratory investigation of biochar-modified asphalt mixture. *Transp. Res. Rec. J. Transp. Res. Board* **2014**, *2445*, 56–63. [CrossRef]

36. AASHTO. *Standard Specification for Performance-Graded Asphlat Binder (m320-10)*; American Association of State Highway and Transportation Officials: Washington, DC, USA, 2013.

37. Wang, Z.; Dai, Q.; Guo, S. Laboratory performance evaluation of both flake graphite and exfoliated graphite nanoplatelet modified asphalt composites. *Constr. Build. Mater.* **2017**, *149*, 515–524. [CrossRef]

38. You, L.; You, Z.; Dai, Q.; Zhang, L. Assessment of nanoparticles dispersion in asphalt during bubble escaping and bursting: Nano hydrated lime modified foamed asphalt. *Constr. Build. Mater.* **2018**, *184*, 391–399. [CrossRef]

39. AASHTO. *Standard Method of Test for Viscosity Determination of Asphalt Binder Using Rotational Viscometer (t 316-13)*; American Association of State Highway and Transportation Officials: Washington, DC, USA, 2013.

40. You, L.; You, Z.; Yang, X.; Ge, D.; Lv, S. Laboratory testing of rheological behavior of water-foamed bitumen. *J. Mater. Civ. Eng.* **2018**, *30*, 04018153. [CrossRef]

41. Lv, S.; Wang, S.; Guo, T.; Xia, C.; Li, J.; Hou, G. Laboratory evaluation on performance of compound-modified asphalt for rock asphalt/styrene–butadiene rubber (sbr) and rock asphalt/nano-CaCO3. *Appl. Sci.* **2018**, *8*, 1009. [CrossRef]

42. AASHTO. *Standard Method of Test for Determining the Rheological Properties of Asphalt Binder Using a Dynamic Shear Rheometer (dsr) (t 315-12)*; American Association of State Highway and Transportation Officials: Washington, DC, USA, 2013.

43. Ge, D.; Yan, K.; You, L.; Wang, Z. Modification mechanism of asphalt modified with sasobit and polyphosphoric acid (ppa). *Constr. Build. Mater.* **2017**, *143*, 419–428. [CrossRef]

44. AASHTO. *Effect of Heat and Air on a Moving Film of Asphalt Binder (Rolling Thin-film Oven Test)*; American Association of State Highway and Transportation Officials: Washington, DC, USA, 2013.

45. AASHTO. *Standard Practice for Accelerated Aging of Asphlat Binder Using a Pressurized Aging Vessel (pav)*; American Association of State Highway and Transportation Officials: Washington, DC, USA, 2013.

46. AASHTO. *Determining the flexural creep stiffness of asphalt binder using the bending beam rheometer (bbr) (t313-12)*; American Association of State Highway and Transportation Officials: Washington, DC, USA, 2013.

47. Yao, H.; You, Z.; Li, L.; Goh, S.W.; Mills-Beale, J.; Shi, X.; Wingard, D. Evaluation of asphalt blended with low percentage of carbon micro-fiber and nanoclay. *J. Test. Eval.* **2013**, *41*, 278–288. [CrossRef]

48. Peng, C.; Yu, J.; Dai, J.; Yin, J. Effect of zn/al layered double hydroxide containing 2-hydroxy-4-n-octoxy-benzophenone on uv aging resistance of asphalt. *Adv. Mater. Sci. Eng.* **2015**, *2015*. [CrossRef]

49. Peng, C.; Dai, J.; Yu, J.; Yin, J. Intercalation of p-methycinnamic acid anion into zn-al layered double hydroxide to improve uv aging resistance of asphalt. *AIP Adv.* **2015**, *5*, 027133. [CrossRef]